

## Determination of the microplastic content in Mediterranean benthic macrofauna by pyrolysis-gas chromatography-tandem mass spectrometry

Albignac Magali <sup>1</sup>, Ghiglione Jean François <sup>2</sup>, Labrune Céline <sup>3</sup>, ter Halle Alexandra <sup>1,\*</sup>

<sup>1</sup> CNRS, Université de Toulouse, Laboratoire des Interactions Moléculaires et Réactivité Chimique et Photochimique (IMRCP), UMR 5623, Toulouse, France

<sup>2</sup> CNRS, Sorbonne Université, Laboratoire d'Océanographie Microbienne (LOMIC), UMR 7621, Observatoire Océanologique de Banyuls, Banyuls sur mer, France

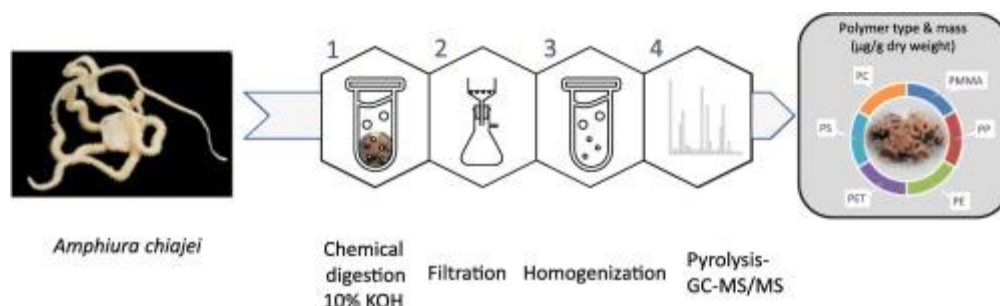
<sup>3</sup> CNRS, Sorbonne Université, Laboratoire d'Ecogéochimie des Environnements Benthiques (LECOB), UMR 8222, Observatoire Océanologique de Banyuls, Banyuls sur mer, France

\* Corresponding author : Alexandra ter Halle, email address : [alexandra.ter-halle@cirs.fr](mailto:alexandra.ter-halle@cirs.fr)

### Abstract :

The Mediterranean Sea water bodies are ones of the most polluted, especially with microplastics. As the seafloor is the ultimate sink for litter, it is considered a hotspot for microplastic pollution. We provide an original analytical development based on the coupling of tandem mass spectrometry to pyrolysis-gas chromatography to improve the detection of plastic contamination in marine organisms. Due to the high selectivity of the mass spectrometer, a straightforward sample preparation consists uniquely of potassium hydroxide digestion. The quantification of six common polymers is possible in one run. The method was applied to analyze the plastic content from 500  $\mu\text{m}$  down to 0.7  $\mu\text{m}$  in the whole body of seven benthic species with variable feeding modes. Plastic was detected in all samples, with an almost systematic detection of polypropylene and polyethylene. Our method presents a major development in determining the levels of plastic contaminations in samples with rich organic matter content.

### Graphical abstract



---

## Highlights

► Quantification of microplastics in marine organisms down to 0.7  $\mu\text{m}$  by pyrolysis-gas chromatography–tandem mass spectrometry. ► A one-step sample preparation consisting of chemical digestion was utilized. ► Six distinct polymer contents were determined in one run. ► The total polymer contents varied greatly from one organism to the other and was between 105 and 7780  $\mu\text{g/g dw}$ . ► The PE, PET and PS polymers were detected the most often.

48 **Introduction**

49

50 Plastic loads are increasing in marine ecosystems worldwide (Barnes et al. 2009),  
51 and the Mediterranean Sea is one of the most affected marine basins (Consoli et al., 2020;  
52 (Galgani et al., 1996). Macrolitter densities that exceeded  $10^5$  items per  $\text{km}^2$  were  
53 recorded near metropolises (Galgani et al., 2000). Microplastic concentrations (less than 5  
54 mm) on the seafloor, which are considered hotspots of accumulation, can reach up to 1.9  
55 million pieces per  $\text{m}^2$  (Kane et al., 2020).

56 An initial explanation for microplastic littering is that the litter is transported to the  
57 seafloor by vertical settling from surface accumulations and is driven by the density of  
58 microplastics. With biofouling, the buoyancy of microplastics is altered, and all types of  
59 plastic can sink—whether they are initially buoyant or not (Kooi et al., 2017). Whereas  
60 macrolitter sinking may be associated with dense downcanyon flows in the

61 Mediterranean (de Madron et al., 2017; (Tubau et al., 2015), microplastic sedimentation  
62 in the deep sea is driven more by near-bed thermohaline currents (Kane et al., 2020). In  
63 coastal areas, seasonal changes in river flow rate and related turbidity currents also  
64 considerably impact the spatial dispersion of litter (Angiolillo et al., 2021).

65 Microplastic hotspots of are also likely hotspots for marine life, as has been shown  
66 from the sea surface microlayer (Ghiglione and Laudet, 2020) to deep-sea sediment (Hall,  
67 2002; (Kane et al., 2020). Marine biota interact with microplastics in several ways, and  
68 this leads to a reduction in feeding and depletion in energy stores but also causes toxicity,  
69 carcinogenesis, endocrine disruption and physical harm with knock-on effects for  
70 fecundity and growth (Galloway et al., 2017). After sedimentation, microplastics are  
71 available for many benthic species to feed on, such as detritivores and filter-feeding  
72 species (Valente et al., 2020). This potentially impacts the biodiversity throughout marine  
73 life, as the benthic community plays an important role in providing resources and  
74 ecosystem services (Danovaro et al., 2020; (Manea et al., 2020). The extent of the  
75 impacts of plastic pollution on Mediterranean ecosystems is poorly estimated, whereas  
76 the Mediterranean Sea is a biodiversity hotspot with high levels of endemism (Coll et al.,  
77 2010). Monitoring litter-benthic community interactions is largely hampered by  
78 difficulties in sampling and the necessary costs (Angiolillo et al., 2021; (Valente et al.,  
79 2020), which is why the interactions are poorly described even if all reported studies  
80 declare that a quasi-systematic of plastic occurs in individuals (Anastasopoulou et al.,  
81 2013).

82 In general, microplastics that are larger than 500  $\mu\text{m}$  are visually detected and  
83 identified by Fourier Transform Infrared Spectroscopy (FT-IR). There are very few  
84 publications that compare microplastics that are smaller than 150  $\mu\text{m}$ . The latest  
85 spectroscopic developments allow limits of tens of microns to be reached (Schwaferts et  
86 al., 2019), but the detection of the particles is strongly impacted by residual organic  
87 matter. This is solved by intensive sample preparations, which are time-consuming and  
88 costly forms of analysis that involve risks including altering and losing some  
89 microplastics and increasing cross contamination. In this context, pyrolysis-gas  
90 chromatography–mass spectrometry (Py-GC–MS) appears to be a very promising  
91 technique, even if its developments are very recent (Yakovenko et al., 2020). The use of  
92 Py-GC–MS does not have size limitations, and the selectivity of the mass spectrometry  
93 offers the possibility to simplify the sample preparation. The use of Py-GC–MS is

94 promising in terms of reducing the time of analysis because several polymers are detected  
95 in one run.

96 In addition to all these promising aspects, there are some consequent obstacles with  
97 the use of Py-GC–MS (Pico and Barcelo, 2020; (Yakovenko et al., 2020). Two recent  
98 studies with important developments resulted, for the first time, in achieving the  
99 following robust methods: one for the analysis of biosolids (Okoffo et al., 2020) and the  
100 other for seafood samples (Ribeiro et al., 2020). Even if a less intensified purification of  
101 the sample is obtained through the use of Py-GC–MS, this step is still important. Okoffo  
102 et al. (2020) opted for pressurized liquid extraction, and the remaining organic matter was  
103 eliminated during Py-GC–MS analysis using a two-step pyrolysis program (organic  
104 matter removal at 300 °C followed by pyrolysis at 650 °C). Ribeiro et al. (2020) proposed  
105 a more intensified sample purification that involved alkaline digestion followed by  
106 pressurized liquid extraction, and they skipped the decomposition step at 300 °C. Here,  
107 we introduce the use of tandem mass spectrometry (Py-GC–MS/MS) to enhance the  
108 detection performance, thus permitting a simpler sample preparation using alkaline  
109 digestion alone. This study aimed to demonstrate that Py-GC–MS/MS is a fast and  
110 reliable tool for microplastic quantification down to 0.7 µm in marine organisms. Here,  
111 we provide the first assessment of microplastic content in Mediterranean benthic  
112 organisms for a selection of 6 different polymers.

113

## 114 **2. Materials and Methods**

### 115 **2.1. Chemicals and Reference Materials.**

116 A total of six polymers were targeted. They were chosen among the most abundant  
117 polymers in the marine environment, namely, high density polyethylene (PE),  
118 poly(methyl methacrylate) (PMMA), polyethylene terephthalate (PET), polycarbonate  
119 (PC), polystyrene (PS), and polypropylene (PP). The first three polymers were purchased  
120 from Sigma–Aldrich (St. Louis, MO, USA) and the three others were from Goodfellow  
121 Group (Huntingdon, United Kingdom). These polymer standards were used to optimize  
122 the mass spectrometry conditions and to prepare standards for external calibration. The  
123 external calibration was performed with a mix of polymers diluted in a calcined  
124 powdered glass microfiber filter (GF/D diameter 47 mm; Whatman® Sigma–Aldrich, St.  
125 Louis, MO, USA).

126

127

## 128 **2.2. Sample Collection and Processing.**

129 All glassware was calcined at 550 °C for 2 hours before use in an incinerator oven  
130 (Nabertherm™ LV052K1RN1). Glass fiber filters were calcined at 600 °C for 2 hours  
131 before use. Benthic organisms were sampled on the northwestern Mediterranean seafloor  
132 from the R/V Nereis II. Specimens sampled with a van veen grab were sorted and stored  
133 in a clean metallic bowl on board. At the laboratory, the specimen were identified and  
134 placed in calcined glass vials that were closed with a cap, which was equipped with a  
135 polytetrafluoroethylene (PTFE) opercula. The details of the GPS location and sampling  
136 depth of each organism are given in Table 1. A sampling control consisted of opening a  
137 calcined glass vial that contained calcined quartz fiber for approximately the same period  
138 of time it took to manipulate the animals both onboard and at the laboratory. The quartz  
139 fiber was analyzed by Py-GC-MS/MS similar to the samples. In the laboratory, all  
140 animals were freeze-dried and weighed. Under the hood, the animals were transferred to  
141 30 mL glass flasks equipped with glass caps. A ratio of 80 mL per gram of dry animal of  
142 10% potassium hydroxide aqueous solution prefiltered was added. The solution was  
143 previously filtered in a closed glass unit from Vagner Glasses Company (Toulouse) on a  
144 calcined 47 mm diameter membrane with a porosity of 0.45 µm (PTFE Omnipore™, from  
145 Sigma-Aldrich, St. Louis, MO, USA) to remove any potential plastic contamination. For  
146 the chemical digestion, the flasks were placed in a shaker incubator (Eppendorf®  
147 ThermoMixer® C, Sigma-Aldrich, St. Louis, MO, USA) for 48 h at 40 °C with  
148 continuous agitation (500 rpm). A similar flask with potassium hydroxide solution and no  
149 sample was used as a procedural blank. Once the digestion was completed, the samples  
150 were removed from the incubator and prefiltered on 500 µm stainless steel filter grids  
151 (Negofiltre, Moret Loing Et Orvanne, France). The solution was then filtered under  
152 vacuum with a closed glass unit onto a calcined glass microfiber filter, GF/F diameter 47  
153 mm or 21 mm Whatman® (Sigma-Aldrich, St. Louis, MO, USA). Filters were stored in  
154 glass Petri dishes before cryogrinding using the SPEX® SamplePrep 6775 Freezer/Mill  
155 cryogenic Grinder (Delta Labo, Avignon) with the program: precool 2 min ; run 1min ;  
156 cool 2 min ; cycles 15 ; cps 15. A sub-sample of 2 mg was precisely weighted in a  
157 microscale with a 10<sup>-5</sup> g precision (Micro Balance from Sartorius, MCE225P-2S00-A  
158 Cubis®-II Semi) on quartz tubes that were freshly calcined at 1000°C with the pyrolysis

159 probe using the “clean” program. A sub-sample of 2 mg was precisely weighted in a  
 160 microscale with a 10<sup>-5</sup> g precision (Micro Balance from Sartorius, MCE225P-2S00-A  
 161 Cubis®-II Semi) on quartz tubes that were freshly calcined at 1000°C with the pyrolysis  
 162 probe using the “clean” program.

163 **Table 1. List of the benthic organisms that were sampled in the northwestern**  
 164 **Mediterranean and analyzed for microplastic contents. The corresponding feeding**  
 165 **modes, sampling depths and coordinates are also given.**

166

<b>Taxa</b>	<b>Phylum</b>	<b>Feeding modes</b>	<b>Depth (m)</b>	<b>Coordinates (WGS84)</b>
<i>Glandiceps talaboti</i>	Enteropneusta	Surface and/or Subsurface deposit feeder	43	42°30.50'N 3°09.11'E
<i>Amphiura chiajei</i>	Echinodermata	Surface deposit feeder	43	42°30.50'N 3°09.11'E
<i>Amphiura filiformis</i>	Echinodermata	Surface deposit and/or suspension feeder	43	42°30.50'N 3°09.11'E
<i>Notomastus sp.</i>	Annelida	Subsurface deposit feeder	43	42°30.50'N 3°09.11'E
<i>Fustiaria rubescens</i>	Molluska	Carnivorous	80	42°30.00'N 3°11.40'E
<i>Acanthocardia sp.</i>	Molluska	Suspension feeder	80	42°30.00'N 3°11.40'E
<i>Lanice conchilega</i>	Annelida	Surface deposit feeder and/or suspension feeder	90	42°30.00'N 3°12.60'E

167

168

### 169 **2.3 Py-GC–MS/MS Analysis.**

170 The method parameters for analysis by pyrolysis were achieved using a CDS Pyroprobe®  
 171 6150 from Quad service (Acheres, France) interfaced with a GC–MS/MS triple  
 172 quadrupole TSQ® 9000, GC Trace 1310 from Thermo Fisher Scientific (Villebon sur  
 173 Yvette, France). The gas chromatography column was a TraceGOLD TG-5SilMS from  
 174 Thermo Fisher Scientific. Samples were pyrolyzed at 600 °C for 30 s. The pyrolysis

175 products were transferred at 300 °C at the interface and were injected at 300 °C with a  
176 split ratio of 15:1 (additional data Table SI 1). Multiple reaction monitoring (MRM)  
177 optimizations for collision energy were obtained using Auto SRM 4.0 for Chromeleon  
178 software in liquid injection with a Thermo Scientific™ AI/AS 1310 autosampler. The MS  
179 acquisition/detection parameters are listed in Table SI 2. Chromatograms were integrated  
180 using the Cobra detection algorithm from Chromeleon 7.2.8 software. The external  
181 calibrations were achieved between 25 ng and 1.4 µg with 6 calibration points (Table 2  
182 and SI 3). The range of the calibration depends greatly on the polymer because the  
183 intensity of the indicator compound could vary greatly. The confirmation/quantification  
184 ratios were established with the external standards. For the external calibration  
185 preparation the polymers were first cryo-milled using the SPEX® SamplePrep 6775  
186 Freezer/Mill cryogenic Grinder (Delta Labo, France) with the program: precool 2 min ;  
187 run 1 min ; cool 2 min ; cycles 15 ; cps 15. This inert matrix was prepared from glass  
188 microfiber filters (GF/D diameter 47 mm from Whatman®) cryo-milled (precool 1 min;  
189 run 1 min; cool 1 min; cycles 6; cps 15) and calcined.

190

#### 191 **2.4 Method Validation and Performance**

192 For each polymer analyzed, an indicator compound was selected for quantification. The  
193 analytical limit of detection (LOD) and limit of quantification (LOQ) were determined  
194 for each polymer and were defined as S/N of 3 and of 10 respectively. This limit was  
195 only reached within the calibration range for PE (130 ng). We selected the following  
196 criteria to assess the possibility of determining a peak concentration: 1) the retention time  
197 was within a window of 0.05 min compared to that of the standards, 2) the peak was  
198 above the analytical LOQ, and 3) there was 30% tolerance in the ratio of the ion  
199 transitions. The interday variability will not be discussed as the external calibration  
200 standards and the samples were all analyzed in the same sequence on the same day.  
201 Finally, a polymer was quantified only if the signal was ten times superior to the  
202 procedural and field sampling blanks (Table SI 4) and we did not subtract the signal of  
203 the blank to the determined concentration. If any of the above cited criteria were not  
204 respected, it was specified that the concentration was not determined (n. d.). The  
205 extraction efficiency of the sample preparation was estimated with a positive control that  
206 consisted of the 6 polymers in concentrations ranging from 940 to 4800 ng/ml of KOH  
207 and proceeded with the same steps as those of the preparation and analysis (Table SI 5).



208 To evaluate matrix interferences during pyrolysis or mass spectrometry detection, we  
209 proceeded to perform the standard addition method after cryo-grinding was performed for  
210 the filters, and the samples were spiked at concentrations of 50 to 300  $\mu\text{g/g}$  depending on  
211 the polymers.

## 212 **2.5. Quality Assurance and Quality Control (QA and QC)**

213 A need for stricter QA and QC during method development for microplastic analysis in  
214 biota was discussed earlier, and we integrated the criteria proposed in the present study  
215 (Hermsen et al., 2018). We took special care to minimize contamination during sampling  
216 and during sample preparation in the laboratory. Only glass and metal were used. The  
217 only plastic that was in contact with the sample was the opercula in the cap PTFE for  
218 sample storage, and this opercula is a polymer that does not interfere with the mass  
219 detection of the polymer targeted here. Glass and inox materials were cleaned thoroughly  
220 three times with Milli-Q water and ethanol and then systematically calcined prior to use.  
221 Laboratory coats that were made of 100% cotton were always worn during the analysis  
222 procedures. The work was performed in a fume hood to minimize contamination by  
223 airborne microplastics. Whenever the samples were not processed, they were stored in  
224 closed glass units. The glass fiber filters were also calcined and stored in glass petri  
225 dishes that were wrapped in aluminum foil before use. The quartz tubes that were used  
226 for access into the pyrolysis chamber were cleaned at 1000  $^{\circ}\text{C}$  for 30 s immediately  
227 before being used and were not stored. The samples in the quartz tube were weighed to  
228 minimize airborne contamination, as the tubes were placed in a metal sample holder that  
229 was stored in a glass unit with a glass cover. All solvents (water, ethanol, or potassium  
230 hydroxide solution) were prefiltered on PTFE (0.45  $\mu\text{m}$ , Omnipore<sup>TM</sup>, from Sigma–  
231 Aldrich, St. Louis, MO, USA). The glass microfiber filters were prepared via an  
232 optimized calcination (from room temperature to 500  $^{\circ}\text{C}$  at a rate of 80 $^{\circ}\text{C}/\text{hour}$  with hold  
233 of 30 hours at 500 $^{\circ}\text{C}$  using a LV 5/11 furnace from Nabertherm®).

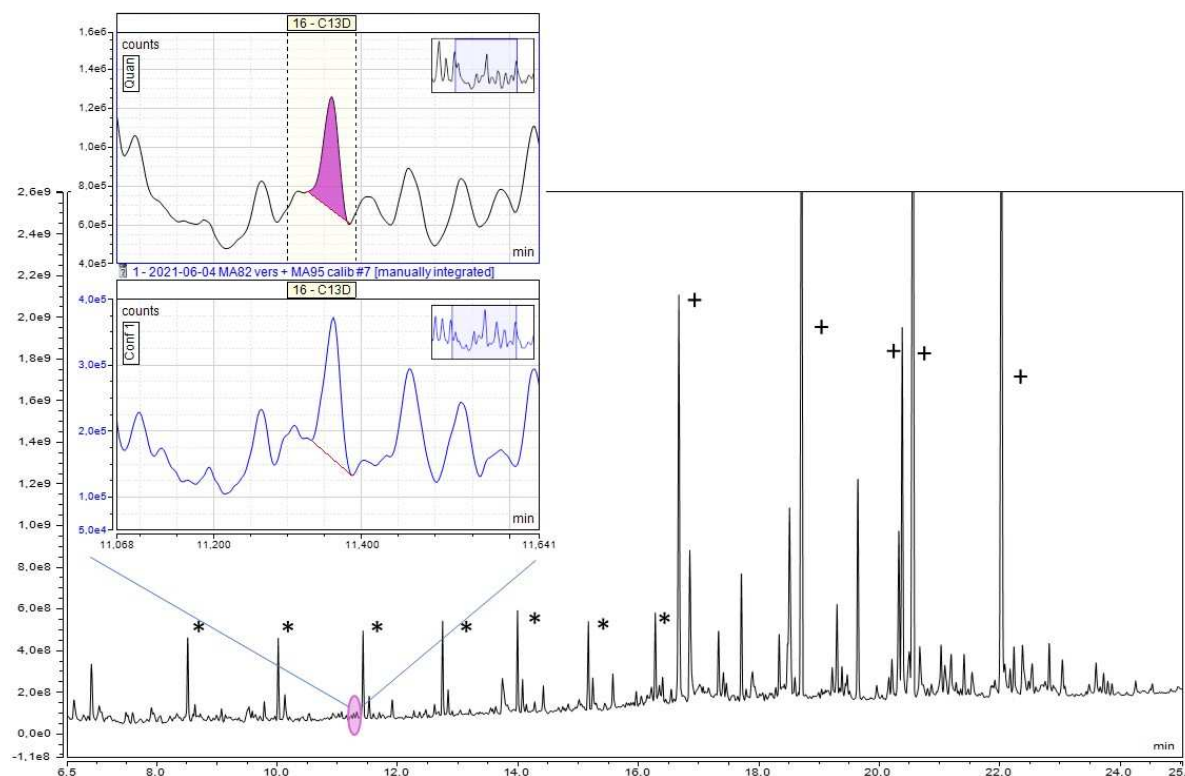
## 234 **3. Results and Discussion**

### 235 **3.1. Indicator compound detection and quantification**

236 The method proposed for the identification and quantification of the six targeted  
237 polymers (PMMA, PP, PE, PET, PS and PC) is new as it is the first development of  
238 tandem mass spectrometry coupled to pyrolysis. The high selectivity of the triple  
239 quadrupole allows to shorten the number of steps of the sampling preparation compared  
240 to what was proposed with a simple quadrupole (Ribeiro et al., 2020). Because PVC

241 products of pyrolysis are aromatic molecules (like benzene, naphthalene ...) and because  
242 they are not specific (there are interferences from organic matter): we excluded this  
243 polymer from the study. For PS, we selected the PS trimer as an indicator compound, as  
244 in most recent studies (Yakovenko et al., 2020). Styrene cannot be used because it is  
245 often a product of natural organic matter pyrolysis (Dierkes et al., 2019; (Fischer and  
246 Scholz-Bottcher, 2017; (Zhou et al., 2019). The specific detection of PE has already been  
247 discussed considerably because biogenic materials such as natural fats (e.g., fish protein)  
248 and waxes are rich in long alkyl chains. They produce n-alkanes and n-alkenes during  
249 pyrolysis (Dierkes et al., 2019; (Fischer and Scholz-Bottcher, 2017; (Scholz-Bottcher et  
250 al., 2013), which are common products in the pyrolytic decomposition of PE. The  
251 selection of an indicator compound among these two families was excluded if there was  
252 no intensive sample purification (Okoffo et al., 2020; (Ribeiro et al., 2020). Thus, we  
253 opted to use an indicator compound among the n-alkadienes, which are very specific to  
254 PE pyrolysis but formed to a much lesser extent (Yakovenko et al., 2020). In this study  
255 we selected the congener with 13 carbon atoms (Table 2). In the samples analyzed, we  
256 systematically detected PE in the MS/MS mode. The presence of PE was effective  
257 because all 3 congeners (the succession of n-alkadienes, n-alkene and n-alkane) were  
258 present with an n between 8 and 17. As a demonstration, we reported the signal in the full  
259 scan of one sample (Figure 1). The pyrochromatogram is very complex, but the  
260 characteristic shape of PE appears in the full scan with the n-alkenes signal (marked with  
261 a star in Figure 1). Some fatty acid esters were also present in important proportions and  
262 originated from residual organic tissues after chemical digestion. In the inset of Figure 1,  
263 the detection of the indicator compound, the n-alkadiene with 13 carbon atoms, is  
264 possible with the use of MS/MS. In this insert, we can see that in addition to the indicator  
265 compound, we detected many other peaks in MS/MS. Many peaks can be detected in  
266 MS/MS (MRM mode) because they have the same transitions as the ones monitored for  
267 the C13 target compound which is rather common among hydrocarbon derivatives but the  
268 transition ratios are distinct even for structural isomers. All those peaks are hydrocarbons  
269 with various unsaturated components and ramifications and are always formed during PE  
270 pyrolysis (Sojak et al., 2007). The interference of PE pyrolysis from organic matter,  
271 especially with regards of lipids, is a very complex problem which was recently  
272 investigated in details (Rauert et al., 2022). In the present study we have considered the  
273 ratio C13/C14 as a validation criterion with a tolerance of 30% compared to the ratios  
274 recorded for the external standards. Work is under progress to further understand PE

275 pyrolysis and interferences with the matrix investigating several indicator compounds  
276 (the ratios recorded for the samples are presented in figure SI 1). In a recent review paper,  
277 we argued for the choice of indicator compound selections for the other polymers  
278 (Yakovenko et al., 2020).



279  
280

281 Figure 1: Full scan analysis of the *Amphiura filiformis* sample. The stars mark the peaks  
282 of the n-alkene congeners; they are the main products of pyrolytic PE decomposition. The  
283 peaks marked with a cross are fatty acid esters and remains of the tissues of the animals  
284 after chemical digestion. In the inset box, the signal of the selected indicator compound  
285 of PE is presented in the MS/MS; we chose the alkadiene congener with 13 carbon atoms  
286 because its signal was the highest.

### 287 3.2 Sample digestion efficiency and evaluation of polymer integrity

288 We selected a chemical digestion protocol using potassium hydroxide to remove the  
289 organic tissues. The efficiency of this protocol was discussed considerably, and  
290 potassium hydroxide appeared to be a good compromise for obtaining an efficient  
291 purification and preserving the polymers (Dehaut et al., 2016). We observed that even if  
292 the organisms sampled were very distinct in terms of their taxonomic species, size,  
293 weight and feeding modes, the protocol was well adapted to this diversity. The digestion  
294 efficiency was estimated by mass balance; we determined that between 97 and 80% of

295 the samples weight was eliminated. The elementary analysis of the remaining matter  
296 showed less than 0.3 % of organic carbon; we are assuming that the material left after  
297 chemical digestion was mainly inorganic. This is in accordance with the fact that some  
298 organisms were deposit feeders and that they are ingesting sediment particles. The  
299 samples with the lowest digestion efficiencies corresponded to *Glandiceps talaboti* and  
300 *Notomastus* sp., which are subsurface deposit feeders. Such organisms typically process  
301 at least one body weight of sediment daily. As a consequence, their alimentary tract  
302 contains large volumes of sediment that are not eliminated during chemical digestion  
303 (Lopez and Levinton, 1987). These results underlined the importance of the weight-  
304 specific feeding rates to be considered when characterizing the plastic that is ingested by  
305 benthic species.

306 Compared to enzymatic digestion, chemical digestion offers many advantages since it is  
307 very efficient and not expensive, but a disadvantage is the possible alteration of some  
308 polymers. It was recently reported that even if PET was resistant to digestion when  
309 potassium hydroxide was used at 60 °C, smaller particles, such as PET fibers, did not  
310 resist such temperatures; thus, lower temperatures are recommended (Treilles et al.,  
311 2020). For instance, the digestion of seafood samples at 60 °C resulted in 32% recoveries  
312 for PET (Ribeiro and al. 2020). For this reason, chemical digestion was performed at 40  
313 °C. We obtained an extraction procedure efficiency for the six spiked polymers between  
314 82 and 129%, which was within the precision margin of the MS/MS method, so we  
315 estimated that the recoveries were acceptable (Table SI 5).

### 316 **3.3. Method Validation and Performance**

317 To proceed to the fabrication of the external calibration we first cryo-milled the polymer  
318 separately. They were then mixed in an inert glass fiber matrix also previously grinded  
319 and calcined to remove any trace of polymers. The external standards were first prepared  
320 at concentrations ranging from 1 mg.g<sup>-1</sup> to 5 mg.g<sup>-1</sup> and the powder was then diluted by a  
321 factor 10. To obtain the external calibration we prepared 5 dilutions to reach the  
322 calibration range detailed Table SI 3. The repeated injection of an external standard  
323 (N=12) showed a standard deviation below 20% for all polymers considered. We thus  
324 consider the homogenization of the powders was satisfactory. The response was linear  
325 within the calibration range for each polymer with a correlation value (R<sup>2</sup>) greater than  
326 0.85 (Table 2). After digestion and filtration of the samples on glass fiber filters, the  
327 filters were cryo-ground to present good homogeneity, as only a fraction, typically 2 mg,

328 was introduced in the pyrolysis chamber. After cryo-grinding, a sample analyzed in  
329 triplicate showed a standard deviation below 35% for all polymers considered (Table SI  
330 6). We estimated that cryo-grinding was efficient and that the sample was sufficiently  
331 homogeneous. The other samples were analyzed once.

332 The procedural and field blank polymer concentrations are presented in Table SI 4. The  
333 amount of PMMA in the samples was not determined because the concentrations in the  
334 sampling control blank were rather important (4.7  $\mu\text{g/g}$  filter, table SI 4). Further studies  
335 are needed to determine the potential source of contamination and to improve the QA/QC  
336 for this polymer.

337 The potential impact of the remaining matter after chemical digestion on the polymer  
338 analysis was assessed with the standard addition method. The pyrolytic fingerprint of all  
339 the polymers was identical when the polymers were injected as a pure sample or within  
340 the matrix, indicating that the presence or residual organic or inorganic matter did not  
341 interfere with the polymer pyrolysis or the MS/MS detection. The case of PE is  
342 remarkable because some natural organic molecules (like lipids) could thermally  
343 decompose into dienes as it was recently reported (Rauert et al., 2022). In order to ensure  
344 that the remaining matter after sample preparation did not enhance the signal of PE we  
345 used an additional validation criterion based on the recording of two indicator compounds  
346 (the analogues with 13 and 14 carbon atoms). The ratios recorded and compared to the  
347 external standards are reported in Figure SI 1.

348 Table 2: Polymers targeted together with the indicator compound selection and external  
349 calibration characteristics.

<b>Polymer</b>	<b>Indicator compound</b>	<b>Quantification transition (<math>m/z</math>)</b>	<b>External calibration range (<math>\mu\text{g}</math>)</b>	<b>Numbers of point</b>	<b><math>r^2</math></b>
<i>PMMA</i>	methyl methacrylate	100>41	35 to 380 ng	6	0.98
<i>PP</i>	2,4-dimethylhept-1-ene	70>55	30 to 300 ng	5	0.90
<i>PE</i>	1,12-tridecadiene	95>67	130 to 1360 ng	6	0.88
<i>PET</i>	dimethyl terephthalate	163>135	25 to 265 ng	6	0.96

<i>PS</i>	5-hexene-1,3,5-triyltribenzene (styrenetrimer)	207>129	50 to 385 ng	5	0.99
<i>PC</i>	2,2-bis(4'-methoxy-phenyl)propane	241>133	27 to 280 ng	6	0.95

350

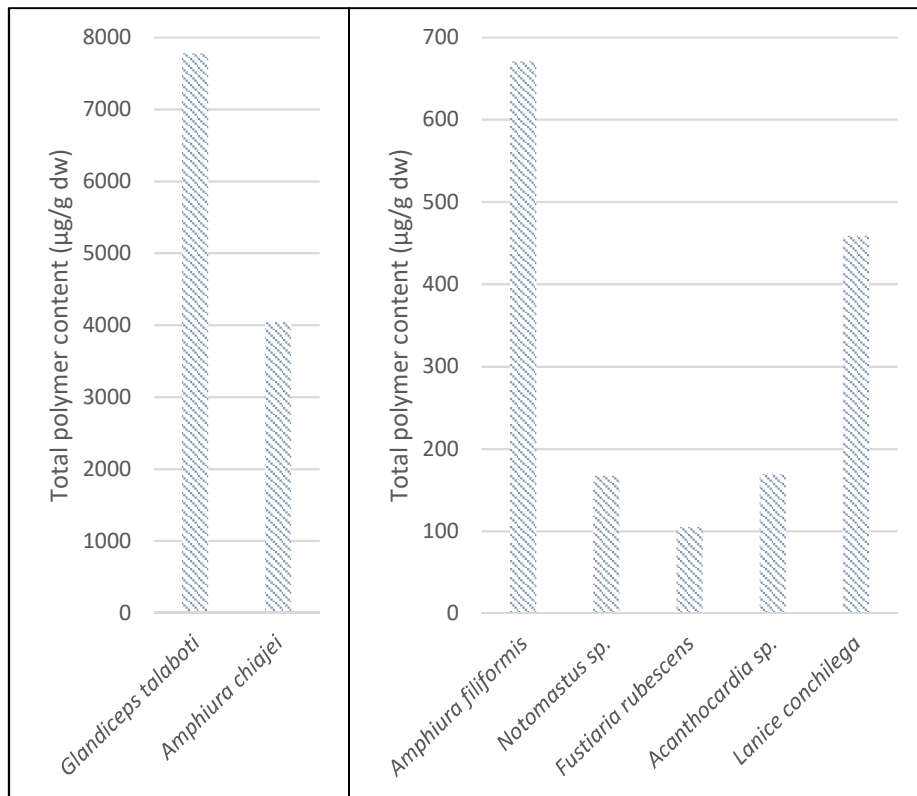
### 351 **3.4. Polymer content in the samples**

352 In general, we systematically detected plastic in the marine benthic animals analyzed.  
 353 The total polymer contents (Figure 2 and Table SI 7) varied from one specimen to  
 354 another and were between 105 and 7780 µg/g dry weight. These margins are within those  
 355 recently determined by Py-GC–MS for seafood (Ribeiro et al., 2020). There is not yet an  
 356 established pattern between the content of plastic in marine organisms and the feeding  
 357 modes, marine habitat or trophic position, even with a large sample set. Microplastic  
 358 accumulation in the marine food chain has been supported by some authors (Carbery et  
 359 al., 2018), while a recent critical review concluded that no plastic biomagnification  
 360 occurred (Walkinshaw et al., 2020). The authors argued that microplastics do not  
 361 translocate from the digestive system into tissues or into circulatory fluid and that  
 362 microplastics are only transitory contaminants with a limited residence time within  
 363 organisms. Nevertheless, the mechanisms of plastic particle ingestion, egestion or  
 364 excretion are still not well understood (Cole et al., 2016). In general, authors assume that  
 365 the residence time of plastic particle in the digestive system is deeply correlated with the  
 366 particle size, shape and rugosity, which are very heterogeneous in the environment and  
 367 could explain the great variations obtained between specimens, in addition to ecological  
 368 or environmental factors.

369 In our study, we collected species with variable feeding modes. *Glandiceps talaboti*,  
 370 *Notomastus* sp. and *Amphiura chiajei* are strict deposit feeders (Buchanan, 1964), while  
 371 *Lanice conchilega* is both a suspension feeder and deposit feeder, depending on the  
 372 environmental conditions (Word, 1990; (Zarkanellas and Kattoulas, 1982). *Amphiura*  
 373 *filiformis* is known to have a main filtering activity (Buchanan, 1964). *Acanthocardia*  
 374 *paucicostata* is a strict suspension feeder, and *Fustiaria rubescens* is a carnivorous  
 375 feeding mainly on foraminifers from sediment surfaces (Gofas et al., 2011). These  
 376 species are known to be good integrators of environmental variation because of their  
 377 reduced mobility. Therefore, their plastic content may be considered a good proxy of the  
 378 plastic content of the environment in the same region, with the limit of the spatial

379 heterogeneity of microplastics on the sea floor. Overall, our results agreed with this  
380 hypothesis by indicating that the type of polymer recovered from benthic animals with  
381 different feeding modes corresponds to the distribution of the polymer in the oceans.  
382 Nonetheless we observed important variation among individuals; this variability was  
383 often reported and is not yet explained (Ribeiro et al., 2020).

384  
385



386  
387  
388  
389

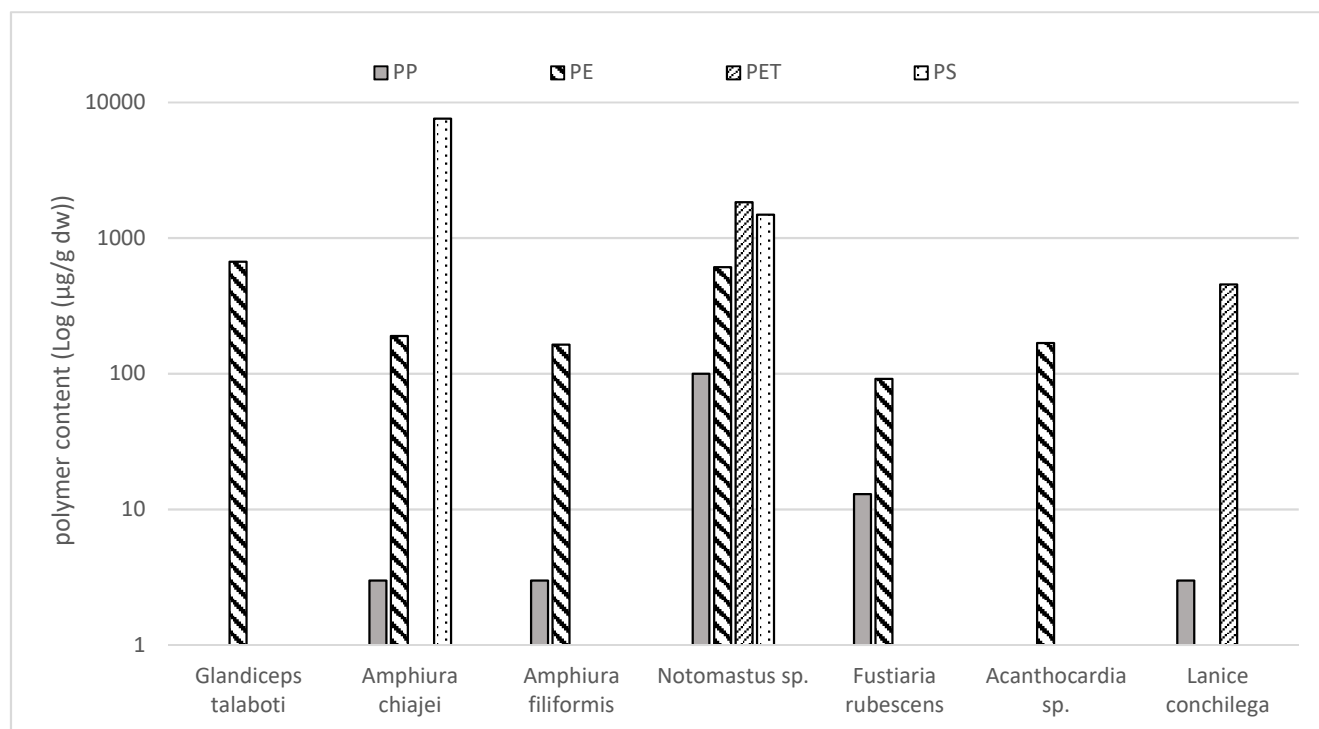
Figure 2: Total polymer content expressed in µg per gram of dry weight (µg/g dw).

390 PE was detected in six samples of the seven analyzed samples (Figure 3) at  
391 concentrations up to 670 µg/g dw for the *Glandiceps talaboti* individual. We noticed that  
392 PE was often present in the largest proportions, often superior to 80% of the total  
393 polymer content. It has been reported that PE was dominant in marine samples with an  
394 average proportion of 42% at the sea surface and with a decrease in abundance through  
395 the water column (Erni-Cassola et al., 2019). Our results agreed with those of Missawi et  
396 al., who reported that PE was dominant in the polychaete worm *Hediste diversicolor* on  
397 the Tunisian coast in the Mediterranean Sea, with important variations among individuals  
398 and sites, whereas PP was detected in lesser proportions than those of PE (Missawi et al.,

399 2020), which is in accordance with the reported concentrations at sea (Erni-Cassola et al.,  
400 2019).

401 *Notomastus sp.* et *Lanice conchilega* presented high contents of PET, which are likely to  
402 be associated with deposit feeders because it is a polymer with a higher density than that  
403 of sea water. Previous studies using spectroscopic characterization emphasized that a  
404 high proportion of PETs were detected in detritivores, which corresponds to plastic fibers  
405 (Renzi et al., 2020). PET fibers have also been detected in high proportions in seafloor  
406 samples (Kane et al., 2020). Figure 3 also shows that *Amphiura chiajei* and *Notomastus*  
407 *sp.* exhibited a high content of PS. They are both deposit feeders and are likely exposed  
408 to denser polymers such as PS. Along the same line, PMMA, which is also known to be  
409 more abundant in the sediment than at its surface (Renzi et al., 2020), has not been  
410 detected in suspension feeders such as *A. filiformis* and *A. paucicostata*. This could be  
411 explained by the relatively high limit of detection for PMMA under our conditions.

412



413

414 Figure 3: Polymer content in the benthic individuals (expressed in µg/g dry weight).

415

#### 416 **Concluding remarks**

417 The study demonstrates that a method based on Py-GC-MS/MS leads to a simplified  
418 sample purification and enables microplastic contents down to 0.7 µm to be determined



419 with good reliability in organisms. Py-GC–MS does not provide information on the color,  
420 shape, or size of microplastics and is complementary to methods that are based on  
421 spectroscopy (Primpke et al., 2020). The use of pyrolysis to quantify microplastics still  
422 involves limitations and areas of improvement that need to be considered before it  
423 becomes a standardized technique. As a first glance, the use of internal standards will  
424 certainly improve the precision of the measurements even if the developments in this  
425 direction present some technical difficulties (Lauschke et al., 2021) that are challenging  
426 because very few isotopic analog resins are commercially available. Other important  
427 undertakings involve achieving a better understanding of matrix interference and the  
428 effect of polymer weathering on the pyrolytic response (Ainali et al., 2021; (Biale et al.,  
429 2021; (Toapanta et al., 2021). The most appealing aspect of Py-GC–MS is that it does not  
430 have size limitations, as there is still very little known about the behavior of small  
431 microplastics in the environment and their interaction with organisms. We emphasize the  
432 promising potential for the use of Py-GC–MS as it involves straightforward sample  
433 preparation, even with complex samples, and the possibility of increasing our capacity to  
434 analyze larger sample sets for environmental assessments. To gain a better understanding  
435 of the interactions of benthic community with plastic pollution, the variation in plastic  
436 concentrations with sediment depth at different locations should be investigated, and this  
437 could be first explored by focusing on a single species with a strict feeding mode.

438

439

440 **References**

- 441
- 442 Ainali, N.M., et al., 2021. Aging effects on low- and high-density polyethylene, polypropylene  
443 and polystyrene under UV irradiation: An insight into decomposition mechanism by Py-GC/MS  
444 for microplastic analysis. *Journal of Analytical and Applied Pyrolysis* 158.  
445 <https://doi.org/10.1016/j.jaap.2021.105207>.
- 446 Anastasopoulou, A., et al., 2013. Plastic debris ingested by deep-water fish of the Ionian Sea  
447 (Eastern Mediterranean). *Deep-Sea Research Part I-Oceanographic Research Papers* 74, 11-13.  
448 <https://doi.org/10.1016/j.dsr.2012.12.008>.
- 449 Angiolillo, M., et al., 2021. Distribution of seafloor litter and its interaction with benthic  
450 organisms in deep waters of the Ligurian Sea (Northwestern Mediterranean). *Sci. Total Environ.*  
451 788. <https://doi.org/10.1016/j.scitotenv.2021.147745>.
- 452 Biale, G., et al., 2021. A Systematic Study on the Degradation Products Generated from  
453 Artificially Aged Microplastics. *Polymers* 13. <https://doi.org/10.3390/polym13121997>.
- 454 Buchanan, J.B., 1964. A comparative study of some features of the biology of *Amphiura filiformis*  
455 and *Amphiura chiajei* (Ophiuroidea) considered in relation to their distribution. *J Mar Biol Ass*  
456 UK 44, 615-624.
- 457 Carbery, M., et al., 2018. Trophic transfer of microplastics and mixed contaminants in the  
458 marine food web and implications for human health. *Environ Int* 115, 400-409.  
459 <https://doi.org/10.1016/j.envint.2018.03.007>.
- 460 Cole, M., et al., 2016. Microplastics Alter the Properties and Sinking Rates of Zooplankton Faecal  
461 Pellets. *Environ. Sci. Technol.* 50, 3239-3246. <https://doi.org/10.1021/acs.est.5b05905>.
- 462 Coll, M., et al., 2010. The Biodiversity of the Mediterranean Sea: Estimates, Patterns, and  
463 Threats. *Plos One* 5. <https://doi.org/10.1371/journal.pone.0011842>.
- 464 Consli, P., et al., 2020. Characterization of seafloor litter on Mediterranean shallow coastal  
465 waters: Evidence from Dive Against Debris (R), a citizen science monitoring approach. *Marine*  
466 *Pollution Bulletin* 150. <https://doi.org/10.1016/j.marpolbul.2019.110763>.
- 467 Danovaro, R., et al., 2020. Towards a marine strategy for the deep Mediterranean Sea: Analysis  
468 of current ecological status. *Marine Policy* 112. <https://doi.org/10.1016/j.marpol.2019.103781>.
- 469 de Madron, X.D., et al., 2017. Deep sediment resuspension and thick nepheloid layer generation  
470 by open-ocean convection. *J Geophys Res-Oceans* 122, 2291-2318.  
471 <https://doi.org/10.1002/2016jc012062>.
- 472 Dehaut, A., et al., 2016. Microplastics in seafood: Benchmark protocol for their extraction and  
473 characterization. *Environ. Pollut.* 215, 223-233. <https://doi.org/10.1016/j.envpol.2016.05.018>.
- 474 Dierkes, G., et al., 2019. Quantification of microplastics in environmental samples via  
475 pressurized liquid extraction and pyrolysis-gas chromatography. *Anal Bioanal Chem* 411, 6959-  
476 6968. <https://doi.org/10.1007/s00216-019-02066-9>.
- 477 Erni-Cassola, G., et al., 2019. Distribution of plastic polymer types in the marine environment; A  
478 meta-analysis. *J. Hazard. Mater.* 369, 691-698. <https://doi.org/10.1016/j.jhazmat.2019.02.067>.
- 479 Fischer, M., Scholz-Bottcher, B.M., 2017. Simultaneous Trace Identification and Quantification of  
480 Common Types of Microplastics in Environmental Samples by Pyrolysis-Gas Chromatography-  
481 Mass Spectrometry. *Environ. Sci. Technol.* 51, 5052-5060.  
482 <https://doi.org/10.1021/acs.est.6b06362>.
- 483 Galgani, F., et al., 2000. Litter on the sea floor along European coasts. *Marine Pollution Bulletin*  
484 40, 516-527. [https://doi.org/10.1016/s0025-326x\(99\)00234-9](https://doi.org/10.1016/s0025-326x(99)00234-9).
- 485 Galgani, F., et al., 1996. Accumulation of debris on the deep sea floor off the French  
486 Mediterranean coast. *Mar Ecol Prog Ser* 142, 225-234. <https://doi.org/10.3354/meps142225>.
- 487 Galloway, T.S., et al., 2017. Interactions of microplastic debris throughout the marine  
488 ecosystem. *Nat Ecol Evol* 1. <https://doi.org/10.1038/s41559-017-0116>.
- 489 Ghiglione, J.F., Laudet, V., 2020. Marine Life Cycle: A Polluted Terra Incognita Is Unveiled.  
490 *Current Biology* 30, R130-R133. <https://doi.org/10.1016/j.cub.2019.11.083>.
- 491 Gofas, S., et al. (2011) *Moluscos marinos de Andalucia*.

492 Hall, S.J., 2002. The continental shelf benthic ecosystem: current status, agents for change and  
493 future prospects. *Environmental Conservation* 29, 350-374.  
494 <https://doi.org/10.1017/s0376892902000243>.

495 Hermesen, E., et al., 2018. Quality Criteria for the Analysis of Microplastic in Biota Samples: A  
496 Critical Review. *Environ. Sci. Technol.* 52, 10230-10240.  
497 <https://doi.org/10.1021/acs.est.8b01611>.

498 Kane, I.A., et al., 2020. Seafloor microplastic hotspots controlled by deep-sea circulation. *Science*  
499 368, 1140-+. <https://doi.org/10.1126/science.aba5899>.

500 Kooi, M., et al., 2017. Ups and Downs in the Ocean: Effects of Biofouling on Vertical Transport of  
501 Microplastics. *Environ. Sci. Technol.* 51, 7963-7971. <https://doi.org/10.1021/acs.est.6b04702>.

502 Lauschke, T., et al., 2021. Evaluation of poly(styrene-d5) and poly(4-fluorostyrene) as internal  
503 standards for microplastics quantification by thermoanalytical methods. *Journal of Analytical*  
504 *and Applied Pyrolysis* 159. <https://doi.org/10.1016/j.jaap.2021.105310>.

505 Lopez, G.R., Levinton, J.S., 1987. Ecology of deposit-feeding animals in marine-sediments.  
506 *Quarterly Review of Biology* 62, 235-260. <https://doi.org/10.1086/415511>.

507 Manea, E., et al., 2020. Towards an Ecosystem-Based Marine Spatial Planning in the deep  
508 Mediterranean Sea. *Sci. Total Environ.* 715. <https://doi.org/10.1016/j.scitotenv.2020.136884>.

509 Missawi, O., et al., 2020. Abundance and distribution of small microplastics (<= 3  $\mu$  m) in  
510 sediments and seaworms from the Southern Mediterranean coasts and characterisation of their  
511 potential harmful effects. *Environ. Pollut.* 263. <https://doi.org/10.1016/j.envpol.2020.114634>.

512 Okoffo, E.D., et al., 2020. Identification and quantification of selected plastics in biosolids by  
513 pressurized liquid extraction combined with double-shot pyrolysis gas chromatography-mass  
514 spectrometry. *Sci. Total Environ.* 715. [https://doi.org/ARTN136924](https://doi.org/ARTN13692410.1016/j.scitotenv.2020.136924)  
515 [10.1016/j.scitotenv.2020.136924](https://doi.org/ARTN13692410.1016/j.scitotenv.2020.136924).

516 Pico, Y., Barcelo, D., 2020. Pyrolysis gas chromatography-mass spectrometry in environmental  
517 analysis: Focus on organic matter and microplastics. *Trac-Trend Anal Chem* 130.  
518 <https://doi.org/ARTN11596410.1016/j.trac.2020.115964>.

519 Primpke, S., et al., 2020. Comparison of pyrolysis gas chromatography/mass spectrometry and  
520 hyperspectral FTIR imaging spectroscopy for the analysis of microplastics. *Anal Bioanal Chem*  
521 412, 8283-8298. <https://doi.org/10.1007/s00216-020-02979-w>.

522 Rauert, C., et al., 2022. Extraction and Pyrolysis-GC-MS analysis of polyethylene in samples with  
523 medium to high lipid content. *Journal of Environmental Exposure Assessment* 1, 13.  
524 <https://doi.org/10.20517/jeea.2022.04>.

525 Renzi, M., et al., 2020. Chemical composition of microplastic in sediments and protected  
526 detritivores from different marine habitats (Salina Island). *Marine Pollution Bulletin* 152.  
527 <https://doi.org/10.1016/j.marpolbul.2020.110918>.

528 Ribeiro, F., et al., 2020. Quantitative Analysis of Selected Plastics in High-Commercial-Value  
529 Australian Seafood by Pyrolysis Gas Chromatography Mass Spectrometry (vol 54, pg 9408,  
530 2020). *Environ. Sci. Technol.* 54, 13364-13364. <https://doi.org/10.1021/acs.est.0c05885>.

531 Scholz-Bottcher, B.M., et al., 2013. An 18th century medication "Mumia vera aegyptica" - Fake  
532 or authentic? *Organic Geochemistry* 65, 1-18.  
533 <https://doi.org/10.1016/j.orggeochem.2013.09.011>.

534 Schwaferts, C., et al., 2019. Methods for the analysis of submicrometer- and nanoplastic  
535 particles in the environment. *Trends Anal. Chem.* 112, 52-65.  
536 <https://doi.org/10.1016/j.trac.2018.12.014>.

537 Sojak, L., et al., 2007. High resolution gas chromatographic-mass spectrometric analysis of  
538 polyethylene and polypropylene thermal cracking products. *Journal of Analytical and Applied*  
539 *Pyrolysis* 78, 387-399. <https://doi.org/10.1016/j.jaap.2006.09.012>.

540 Toapanta, T., et al., 2021. Influence of surface oxidation on the quantification of polypropylene  
541 microplastics by pyrolysis gas chromatography mass spectrometry. *Sci. Total Environ.* 796.  
542 <https://doi.org/10.1016/j.scitotenv.2021.148835>.

543 Treilles, R., et al., 2020. Impacts of organic matter digestion protocols on synthetic, artificial and  
544 natural raw fibers. *Sci. Total Environ.* 748. <https://doi.org/ARTN 141230>  
545 [10.1016/j.scitotenv.2020.141230](https://doi.org/10.1016/j.scitotenv.2020.141230).  
546 Tubau, X., et al., 2015. Marine litter on the floor of deep submarine canyons of the  
547 Northwestern Mediterranean Sea: The role of hydrodynamic processes. *Prog Oceanogr* 134,  
548 379-403. <https://doi.org/10.1016/j.pocean.2015.03.013>.  
549 Valente, T., et al., 2020. Macro-litter ingestion in deep-water habitats: is an underestimation  
550 occurring? *Environmental Research* 186. <https://doi.org/10.1016/j.envres.2020.109556>.  
551 Walkinshaw, C., et al., 2020. Microplastics and seafood: lower trophic organisms at highest risk  
552 of contamination. *Ecotoxicology and Environmental Safety* 190.  
553 <https://doi.org/10.1016/j.ecoenv.2019.110066>.  
554 Word, J.Q., 1990. The infaunal trophic index, a functional approach to benthic community  
555 analyses.  
556 Yakovenko, N., et al., 2020. Emerging use thermo-analytical method coupled with mass  
557 spectrometry for the quantification of micro(nano)plastics in environmental samples. *TrAC*  
558 *Trends in Analytical Chemistry* 131, 115979.  
559 <https://doi.org/https://doi.org/10.1016/j.trac.2020.115979>.  
560 Zarkanellas, A.J., Kattoulas, M.E., 1982. The Ecology of Benthos in the Gulf of ThermaTkos,  
561 Greece. *Marine Ecology* 3, 21-39.  
562 Zhou, X.X., et al., 2019. Cloud-Point Extraction Combined with Thermal Degradation for  
563 Nanoplastic Analysis Using Pyrolysis Gas Chromatography-Mass Spectrometry. *Analytical*  
564 *Chemistry* 91, 1785-1790. <https://doi.org/10.1021/acs.analchem.8b04729>.

565

566

567



*Amphiura chiajei*

